DANISH METEOROLOGICAL INSTITUTE

—— SCIENTIFIC REPORT ——

03-06

Impact of NOAA16 and NOAA17 ATOVS AMSU-A radiance data in the DMI-HIRLAM 3D-VAR analysis and forecasting system - January and February 2003

Bjarne Amstrup

COPENHAGEN 2003

Impact of NOAA16 and NOAA17 ATOVS AMSU-A radiance data in the DMI-HIRLAM 3D-VAR analysis and forecasting system — January and February 2003

Bjarne Amstrup

Danish Meteorological Institute

Abstract

This report describes relevant statistics for the satellite observations used and the results from an observing system experiment (OSE) using Advanced TIROS (Television Infra-Red Observation Satellite) Operational Vertical Sounder (ATOVS) brightness temperatures from the polar orbiting satellites NOAA16 and NOAA17 (National Oceanic and Atmospheric Administration) in near real-time in January and February 2003. The reference experiment does not use ATOVS data. All AMSU-A (Advanced Microwave Sounding Unit-A) level 1c data (channels 1 to 10, only) available from locally received data from the DMI Smidsbjerg antenna as well as from the DMI Sdr. Strømfjord/Kangerlussuaq (Greenland) antenna have been used.

An example from November 2002 shows the importance of the first guess check.

Based on observation (obs-) and field verification the impact is positive in this period.

1. Introduction

TOVS/ATOVS data have been assimilated at ECMWF (European Centre for Medium-Range Weather Forecasts), NCEP (National Centre for Environmental Prediction), Météo France, UKMO (United Kingdom Meteorological Office) for a number of years and are considered to be the most important non-conventional data of the observing system (see, e.g., Bouttier and Kelly, 2001). The (A)TOVS-related research and development activities within the HIRLAM (HIgh Resolution Limited Area Model) project also have a long history, dating back to Gustafsson and Svensson, 1988. However, only recently have some HIRLAM operational systems started to use ATOVS in the data-assimilation. The reason is that it has been difficult to get a positive impact when using these data. With the introduction of the HIRLAM 3D-VAR analysis it became possible to use radiances directly instead of derived temperatures by, e.g., a 1-dimensional retrieval from the measured satellite radiances. The first tests showed only a minor impact and some development and checking were necessary in the way data was used as well as some further developments in the analysis system. Furthermore, a first guess check was considered to be necessary before an operational implementation at DMI. Such a check was implemented in the HIRLAM 3D-VAR analysis in December 2001. At DMI ongoing experiments with use of AMSU-A data has taken place since 2001 (see, e.g. (Amstrup, 2001; Schyberg *et al.*, 2003)).

NOAA16 AMSU-A data were included in the pre-operational suite running in parallel with the operational suite in April 2002 and they have been used in the operational suite since December 9th 2002. When NOAA16 data became part of the operational suite, NOAA17 data started to be assimilated in the pre-operational suite. NOAA17 were launched June 24th 2002 and there were not sufficient time (from the first data received locally at DMI in late September 2002 and subsequent testing of the data) to test the data in the pre-operational runs before the DMI-HIRLAM upgrade in December 2002. One of the reasons for the lack of time to test the inclusion of these data is the need to include the data in passive mode in the assimilation system to obtain the necessary statistics in terms of a bias correction file. Here passive mode means that the ATOVS data are processed and the innovations (observation−background, see later) computed but not used in further analysis steps. The present (early 2003) pre-operational suite contains other changes than the use of NOAA17 AMSU-A data and it is accordingly of relevance to make an OSE experiment. The present OSE is a set of experiments of which one uses neither NOAA16 nor NOAA17 data (called NOA), and an experiment using data from both NOAA16 and NOAA17 (called WIA). The observation error covariance matrix used for NOAA17 at DMI is identical to the one used for NOAA16 data.

In order to compare the performance of different data-assimilation experiments the forecasts are verified against observations from European radiosonde and synoptic stations to give an objective evaluation of the experiments. Since the stations involved in this obs-verification cover a limited part of the model domain, the forecasts are also compared with initialized analyses from their own data-assimilation suite (field-verification). The DMI observation- and field-verification packages are used.

Section 2 describes the DMI-HIRLAM 3D-VAR analysis system and forecasting system as well as some changes made during the runs. Section 3 describes briefly the ATOVS AMSU-A instrument and the usage of ATOVS AMSU-A brightness temperatures in the HIRLAM 3D-VAR system as well as some results from passive inclusion of the data prior to and during the real experiment. Section 4 gives some results, and finally a summary of the conclusions drawn from the experiments is given in section 5.

2. DMI-HIRLAM 3D-VAR data-assimilation system

The operational data-assimilation system for DMI-HIRLAM-G has since the end of September 2000 been a 3D-VAR analysis scheme (Gustafsson *et al.*, 2001; Lindskog *et al.*, 2001) and a forecast model (based on reference version 5.x with some local modifications). The DMI system is documented in Sass *et al.* (2002) and the upgrade in December 2002 is documented in Amstrup *et al.* (2003).

The version used here is the HIRLAM 3D-VAR 5.1.2 OpenMP version for NEC. The observation window covers a 3 h span around the analysis time (00, 03, 06, 09, 12, 15, 18 and 21 UTC) except for a 6 h span around the analysis times 06 UTC and 18 UTC before the long forecasts starting from these. For AMDAR/ACARS (Aircraft Meteorological Data Reporting/Aircraft Communication Addressing and Reporting System) aircraft observation data a $\pm\frac{1}{2}$ h observation time window is used. This reduced window for AMDAR/ACARS is a reminence from the use of OI (Optimum Interpolation) analysis since a longer time window often caused along track

analysis increments leading to spurious effects in the following forecast. A standard observation set is used, including synoptic observations, ship observations, (drifting and moored) buoys, pilot balloons, radiosonde data and aircraft data. The run with these observation types is denoted NOA (NO ATOVS) and the run denoted WIA (WIth ATOVS) also uses NOAA16 and NOAA17 AMSU-A brightness temperature data as described in the next section. The first guess field is a 3 h forecast from the preceding data-assimilation cycle except for a 6 h forecast for the analyses at 06 UTC and 18 UTC as mentioned above before the long forecasts starting from these.

The basic model applied in the present parallel experiment is DMI-HIRLAM-G (see Sass *et al.*, (2002) for details) including the changes made with the upgrade made in December 2002 (Amstrup *et al.*, 2003). Furthermore, since January 15th 2003 the resolution of ECMWF sst- and ice-fields has been increased to $0.5°$ instead of $1.0°$. The horizontal resolution of DMI-HIRLAM-G (see Figure 1) is $0.45°$, the number of vertical levels is 40, the number of grid points is 190 202, the time step is 150 s and the lateral boundary values are updated every 3 hours from ECMWF FRAME boundary fields. Note that the number of vertical levels are now 40 compared to the 31 levels used in the former OSE experiments (Amstrup, 2001; Schyberg *et al.*, 2003) with NOAA16 data.
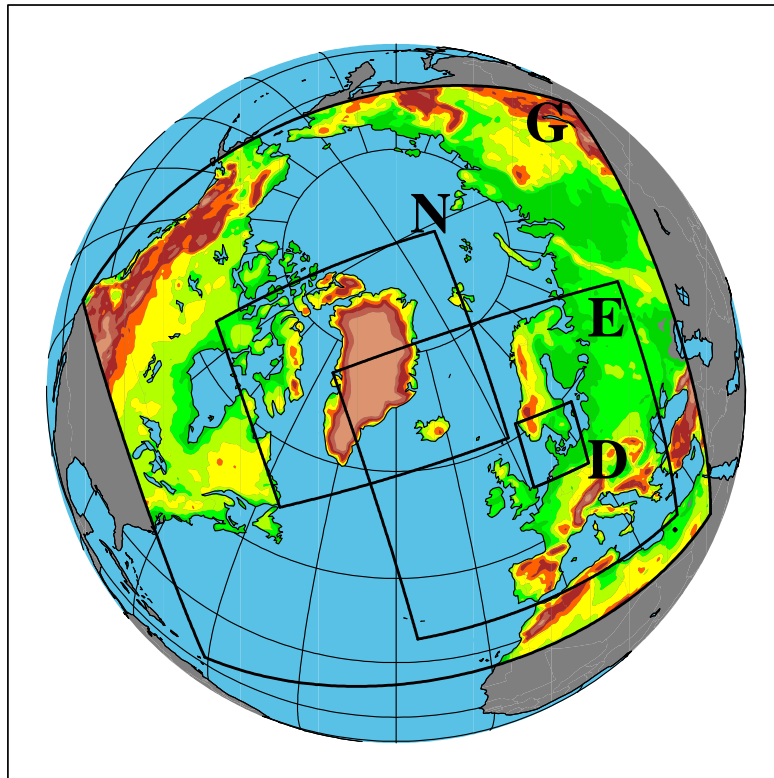
	G	E	D	N
$x_{\text{lon},1}$	$-63.725°$	$-54.275°$	$-36.675°$	$-29.075°$
$y_{\text{lat},1}$	$-37.527°$	$-28.677°$	$-15.177°$	$-5.277°$

Figure 1: Operational DMI-HIRLAM areas and the starting coordinates (south west corner) in the rotated coordinate system with polar coordinates $(P_{\text{lat}}, P_{\text{lon}}) = (0°, 80°)$.

Twice a day (at 00 UTC and 12 UTC reassimilation cycles) the DMI-HIRLAM-G model is restarted from fresh ECMWF analyses using an analysis increment method. The available analysis for the model is interpolated to the grid used for ECMWF data. The difference between interpolation and the new ECMWF analysis is an increment ("large scale increment") which is interpolated to the HIRLAM grid and added to get an updated HIRLAM analysis. Normal HIRLAM cycles then follow (03 UTC, 06 UTC, 09 UTC) in the morning to produce an "up-to-date" status of the atmosphere. In the evening the subsequent analyses are valid at 15 UTC, 18 UTC and 21 UTC, respectively. Using this method ATOVS data are implicitly used even if they are not assimilated into the HIRLAM model since ECMWF uses these data in their analysis system. During the reassimilation cycles, the HIRLAM sst- and ice-fields are updated from the corresponding ECMWF fields.

3. The ATOVS instruments and ATOVS AMSU-A usage in HIRLAM 3D-VAR

The three most recent polar orbiting satellites in the National Oceanic and Atmospheric Administration (NOAA) series, NOAA15, NOAA16 and NOAA17, are carrying a new generation of instruments called ATOVS. The ATOVS instruments are: AMSU-A1/AMSU-A2 (Advanced Microwave Sounding Unit-A), AMSU-B (Advanced Microwave Sounding Unit-B), HIRS/3 (High Resolution Infrared Radiation Sounder/3), and AVHRR/3 (Advanced Very High Resolution Radiometer/3). The instruments provide passive measurements of the radiation emitted from the earth's surface and throughout the atmosphere. The radiances contain temperature as well as humidity information. The AMSU-A instruments used so far in HIRLAM 3D-VAR have 15 channels in total of which 4 (channels 1, 2, 3 and 15) measure in "window" spectral regions and the remaining 11 channels are "temperature sounding" channels. The temperature sounding channels can be used to derive atmospheric temperature profiles from the surface to an altitude of about 40 km. However, areas with precipitation can cause erroneous estimates of the temperature in the lower troposphere and measurements in such areas should not be used without extra precautions, if used at all. The window channels receive energy primarily from the surface and the boundary layer, and can be used, for example, to derive total precipitable water and cloud liquid water. See `http://www2.ncdc.noaa.gov/docs/klm/` for further details on the NOAA15/NOAA16/NOAA17 instruments, and `http://www.ecmwf.int/products/forecasts/d/charts/monitoring/coverage/dcover` for ECMWF usage of HIRS and AMSU radiance data and monitoring of the data.

The data used in the present impact study are data received locally from the Smidsbjerg and Sdr. Strømfjord (Kangerlussuaq) antennas and further processed with the AAPP (ATOVS and AVHRR Processing Package) package (see `http://www.eumetsat.de/en/index.html`): The raw (level 0) data received are processed in 3 steps to level 1c (geo-referenced and calibrated temperatures and albedo) data. The resulting level 1c data, containing brightness temperatures for the 15 AMSU-A channels, are then further processed separately from AAPP to the standard BUFR-format (WMO, 1995). The data from Sdr. Strømfjord have been available since late May 2001 (NOAA16 data) and early December 2002 (NOAA17 data). By receiving the data this way they can easily be made available for assimilation within one hour after the

Table 1: μ and σ (of level 1c (OBS $-$ AN) brightness temperature departure (in K)) for NOAA16 and NOAA17 AMSU-A channels 4 through 10 for January/February 2003. Rows with subscript raw on μ/σ is for uncorrected data and the other rows are for bias corrected data.

sat.↓	chnl.→	4	5	6	7	8	9	10
NOAA16	$\mu_{\mathrm{raw}}/\mathrm{K}$	0.96	0.38	-0.33	-0.03	-0.07	-0.43	-1.19
	$\sigma_{\mathrm{raw}}/\mathrm{K}$	1.57	0.58	0.44	0.40	0.40	0.60	1.32
	$\mu_{\mathrm{bc}}/\mathrm{K}$	0.35	-0.01	-0.01	-0.01	-0.09	-0.11	-0.53
	$\sigma_{\mathrm{bc}}/\mathrm{K}$	1.00	0.37	0.23	0.27	0.44	0.44	0.96
NOAA17	$\mu_{\mathrm{raw}}/\mathrm{K}$	0.88	0.48	-0.50	-0.14	-0.03	-0.55	-1.29
	$\sigma_{\mathrm{raw}}/\mathrm{K}$	1.55	0.67	0.62	0.52	0.35	0.69	1.42
	$\mu_{\mathrm{bc}}/\mathrm{K}$	0.11	-0.02	-0.05	-0.02	0.00	-0.01	0.09
	$\sigma_{\mathrm{bc}}/\mathrm{K}$	0.95	0.38	0.27	0.40	0.34	0.37	0.52

observation time.

The radiative forward model presently used for calculating brightness temperatures is based on RTTOV-7 (Radiative Transfer model for TOVS, release 7), available from from the Numerical Weather Prediction SAF (Satellite Application Facility) (see `http://www.metoffice.com/research/interproj/nwpsaf/index.html` and Saunders *et al.*, 1999). RTTOV-7 is necessary in order to be able to use NOAA17 ATOVS data.

At present a diagonal observation error covariance matrix is used. The values for NOAA16 as well as for NOAA17 are 900 K^2 for channels 1 to 3, 90 K^2 for channel 4, 0.35 K^2 for channels 5 to 8, 0.70 K^2 for channel 9 and 1.40 K^2 for channel 10. The values for channels 1 to 3 should be sufficiently high to minimize the use of data for these channels. The values for channels 9 and 10 are higher than for the channels 5 to 8 because the response function for these channels do have nonnegligible amplitudes above the vertical limit of the DMI-HIRLAM models, 10 hPa (see Figure 2). Climate values are at present used in the radiation transfer model for levels above the vertical limit of the model. It may be considered to use values from the ECMWF model and/or to extend the model upwards for this instead.

The data are thinned in three steps (0.3° and 0.6° intermediate) to 0.9° for NOAA16 and NOAA17 data separately.

The examination that was done for NOAA16 data (Schyberg *et al.*, 2003) showed that the scatter of the difference between observed and modeled brightness temperature varied significantly as a function of latitude. It was therefore decided to have separate bias correction coefficients for three latitude bands: 1) up to 50°N, 2) between 50°N and 65°N, and 3) north of 65°N. With these limits, the number of observations were approximately the same in the three areas – except for the northern band depending on the time of the year due to different ice coverage for different seasons.

Further details concerning assimilation of ATOVS data in the HIRLAM 3D-VAR system can be found in Schyberg *et al.* (2003).

3.1. Statistics.

Figure 3 shows the distribution of the number of innovations within 0.1 K intervals for channels 4 through 10 for NOAA17 data. The "best fit" Gaussian distribution for channels 5 through 10 are also overlayed. The Gaussian distribution are determined by the mean value (μ) of and the variance (σ) of the innovations $y_{\text{raw}}^i - y_{\text{mod}}$:

$$\mu = \frac{1}{N} \sum_{i=1}^{N} \left(y_{\text{raw}}^i - y_{\text{mod}}^i \right)$$

$$\sigma^2 = \frac{1}{N} \sum_{i=1}^{N} \left(y_{\text{raw}}^i - y_{\text{mod}}^i \right)^2 - \mu^2$$

where N is the total number of innovations included. y_{raw} is the actual observed brightness temperature and y_{mod} is the modeled brightness temperature from the forward model. The Gaussian distribution overlayed is then given by

$$\text{Gauss}(\Delta T_{\text{BT}}) = A \exp \left(-\tfrac{1}{2} \left((\Delta T_{\text{BT}} - \mu)/\sigma \right)^2 \right)$$

It is clear from the figure that the distributions are not Gaussians since the data for most of the channels are asymmetric, in particular channels 4, 9 and 10. Figure 4 show the similar distributions for bias corrected innovations for NOAA17. As expected the bias has been reduced for all channels and the fit to a Gaussian has been improved for the channel 4 data. The distribution of channel 9 and 10 data has become closer to being Gaussian. It could be important to get rid of the non-Gaussian data in the first guess check. Figures 5 and 6 show the corresponding figures for NOAA16 data. The same trends except for worse bias corrected data for channel 10 can be seen. The reason for the "shoulder" on the bias corrected data for this channel may be twofold: a) different relations between the "real" weather and the climate values used for the RTTOV model in the period for which the bias correction is made and for (part of) the period considered here, and b) the difference in the position of the upper levels in the newer 40 levels compared to the old 31 levels. Table 1 summarizes the Gaussian fit parameters μ and σ.

The bias correction coefficients for the NOAA17 data are based on passive runs from October 19th to November 12th 2002. For NOAA16 the bias correction coefficients are based on data from the full month of April 2002.

Daily statistics of the difference between actual observed brightness temperatures and modeled from the analysis field for channels 1 to 10 for NOAA16 and NOAA17 are shown in Figures 7 and 8, respectively. The effect of bias correction is clear since both bias and rms in general are much better for the bias corrected data. It can also be seen that the rms-values for channels 1, 2 and 3 are high for both NOAA16 and NOAA17 data.

Figure 9 shows the number of active rtm ATOVS in the 3D-VAR minimization during January and February 2003 for the given analysis cycles. There is in general a reasonable number of active data for the analyses at the asynoptic hours 03 UTC, 15 UTC and 21 UTC and fewer for the analyses at the asynoptic hour 09 UTC. For the synoptic hours the largest number in average is for the 12 UTC analysis hour and the lowest number in average for the 18 UTC analysis hour. The day to day variance in the number of active data is due to the "odd" time interval for a full orbit, namely approximately 100 min. Therefore there is a little more than 14 complete orbits during 24 h.

6

3.2. First guess check

In the days around November 23rd 2002 some problems showed up in the AMSU-A data from NOAA16. It turned out that the first guess check limits used at that time were too high so that some of the poor quality data were used in the minimization in 3D-VAR. Figure 10 show cost function values for the test runs in November 2002 for the 03 UTC and 15 UTC data-assimilation. Note that the "FG NOA/FG WIA/FG WIA ex" cost function values are for the first value in the analyses which are a pure J_o term ($J_b = 0$) and is for the background fields interpolated and possibly modeled to the corresponding observations. The first guess check tests whether the squared difference between the observed value and the modeled value calculated from the first guess fields normalized with the sum of the observation error variance and the background error variance is within 3 given limits (Lindskog *et al.*, 2001). These limits can be set via a namelist variable (rtmbtchklim). The observation are marked as "correct", "probably correct", "probably incorrect" and "incorrect" according to this test. If a brightness temperature is marked "probably incorrect" or "incorrect" it is rejected. If more than one channel in a given scan is rejected for this reason, all channels are rejected. The original limits in the namelist variable rtmbtchklim were (5.0,10.0,12.0). Since the background error variance is somewhat larger than the observation error variance for AMSU-A channels 5 to 9, those limits were too high. A period from November 21 to 26 were rerun with the variables changed to (1.5,3.0,4.5) and (1.0,2.0,3.0), respectively. The first set were still too high whereas the latter set were considered acceptable. Figure 11 show a plot similar to Figure 10 for the runs with the revised set. The number of accepted NOAA16 AMSU-A data were drastically reduced. The number of accepted NOAA17 data were unchanged by the reduction in rtmbtchklim values.

4. Results

We analyses model scores in two ways: a) observation verification (obs-verification), where model forecasts are verified against observations, and b) field verification, where model forecasts are compared with their own verifying analyses on a grid point by grid point basis.

4.1. Observation verification

Figures 12 and 13 show observation verification scores for January 2003 and February 2003, respectively using the standard EWGLAM (European Working Group on Limited Area Modeling) station list and ECMWF analysis data for the screening of observations. The rms-scores are in general better for WIA than NOA for the upper level parameters and for mslp. The bias-scores are more similar. The daily differences in the scores for 48 h forecasts are also considerable for bias-scores as seen in Figures 14 and 15. Note that these figures show bias- and standard deviation scores.

Contingency tables of precipitation accumulated over 12 hours (from 6 to 18 hour forecasts and from 18 to 30 hours) are shown in Tables 2 and 3. The numbers in these tables are obtained by counting the number of observed and predicted precipitation amounts in each of five classes for EWGLAM stations reporting 12 hour accumulated precipitation at 06 UTC and/or 18 UTC. The five precipitation classes are (precipitation amounts in mm): $P1 < 0.2$, $0.2 \leq P2 < 1.0$,

Table 2: Contingency tables of precipitation for January 2003 (6–18 h and 18–30 h forecasts). EWGLAM station list.

NOA 200301 (6–18 h)							WIA 200301 (6–18 h)					
obs→ ↓for	O1	O2	O3	O4	O5	sum	obs→ ↓for	O1	O2	O3	O4	O5	sum
F1	**6989**	405	110	16	**8**	7528	F1	**6911**	417	109	11	**7**	7455
F2	4959	**1360**	673	87	23	7102	F2	5090	**1392**	674	100	30	7286
F3	1621	1429	**2033**	498	140	5721	F3	1561	1365	**2024**	505	134	5589
F4	105	106	396	**307**	189	1103	F4	119	121	398	**282**	181	1101
F5	**21**	28	79	103	**177**	408	F5	**14**	33	86	113	**185**	431
sum	13695	3328	3291	1011	537	21862	sum	13695	3328	3291	1011	537	21862
%FO	51	41	62	30	33	50	%FO	50	42	62	28	34	49

NOA 200301 (18–30 h)							WIA 200301 (18–30 h)					
obs→ ↓for	O1	O2	O3	O4	O5	sum	obs→ ↓for	O1	O2	O3	O4	O5	sum
F1	**6556**	432	146	20	**8**	7162	F1	**6547**	427	119	10	**7**	7110
F2	5195	**1266**	613	92	27	7193	F2	5177	**1321**	654	110	34	7296
F3	1778	1445	**2017**	517	162	5919	F3	1811	1400	**2021**	531	163	5926
F4	137	153	437	**267**	177	1171	F4	138	149	409	**251**	177	1124
F5	**29**	32	78	115	**163**	417	F5	**22**	31	88	109	**156**	406
sum	13695	3328	3291	1011	537	21862	sum	13695	3328	3291	1011	537	21862
%FO	48	38	61	26	30	47	%FO	48	40	61	25	29	47

Table 3: Contingency tables of precipitation for February 2003 (6–18 h and 18–30 h forecasts). EWGLAM station list.

NOA 200302 (6–18 h)							WIA 200302 (6–18 h)					
obs→ ↓for	O1	O2	O3	O4	O5	sum	obs→ ↓for	O1	O2	O3	O4	O5	sum
F1	**7753**	216	70	15	**8**	8062	F1	**7766**	201	60	11	**4**	8042
F2	4170	**736**	260	29	11	5206	F2	4159	**733**	280	36	13	5221
F3	885	589	**874**	207	76	2631	F3	885	606	**871**	196	78	2636
F4	73	63	184	**165**	81	566	F4	67	57	182	**176**	76	558
F5	**17**	14	48	50	**92**	221	F5	**21**	21	43	47	**97**	229
sum	12898	1618	1436	466	268	16686	sum	12898	1618	1436	466	268	16686
%FO	60	45	61	35	34	58	%FO	60	45	61	38	36	58

NOA 200302 (18–30 h)							WIA 200302 (18–30 h)					
obs→ ↓for	O1	O2	O3	O4	O5	sum	obs→ ↓for	O1	O2	O3	O4	O5	sum
F1	**7284**	236	81	16	**5**	7622	F1	**7205**	210	65	17	**4**	7501
F2	4413	**680**	260	34	16	5403	F2	4508	**696**	284	40	17	5545
F3	1099	614	**844**	237	87	2881	F3	1078	630	**847**	237	86	2878
F4	79	73	202	**137**	76	567	F4	86	70	195	**132**	77	560
F5	**23**	15	49	42	**84**	213	F5	**21**	12	45	40	**84**	202
sum	12898	1618	1436	466	268	16686	sum	12898	1618	1436	466	268	16686
%FO	56	42	59	29	31	54	%FO	56	43	59	28	31	54

Table 4: Contingency tables of precipitation for January 2003 (6–18 h and 18–30 h forecasts). Danish station list.

NOA 200301 (6-18 h)							WIA 200301 (6-18 h)						
obs→ ↓for	O1	O2	O3	O4	O5	sum	obs→ ↓for	O1	O2	O3	O4	O5	sum
F1	**446**	32	7	2	**2**	489	F1	**452**	39	3	2	**2**	498
F2	494	**156**	74	4	1	729	F2	480	**151**	70	4	0	705
F3	83	114	**180**	21	5	403	F3	93	112	**194**	28	6	433
F4	2	3	24	**22**	0	51	F4	0	2	17	**15**	0	34
F5	0	0	0	0	**0**	0	F5	0	1	1	0	**0**	2
sum	1025	305	285	49	8	1672	sum	1025	305	285	49	8	1672
%FO	44	51	63	45	0	48	%FO	44	50	68	31	0	49

NOA 200301 (18-30 h)							WIA 200301 (18-30 h)						
obs→ ↓for	O1	O2	O3	O4	O5	sum	obs→ ↓for	O1	O2	O3	O4	O5	sum
F1	**364**	29	8	4	**2**	407	F1	**357**	18	7	1	**2**	385
F2	512	**133**	80	13	3	741	F2	535	**160**	69	10	0	774
F3	144	134	**183**	27	3	491	F3	129	118	**190**	29	5	471
F4	5	9	14	**5**	0	33	F4	4	8	18	**9**	1	40
F5	0	0	0	0	**0**	0	F5	0	1	1	0	**0**	2
sum	1025	305	285	49	8	1672	sum	1025	305	285	49	8	1672
%FO	36	44	64	10	0	41	%FO	35	52	67	18	0	43

Table 5: Contingency tables of precipitation for February 2003 (6–18 h and 18–30 h forecasts). Danish station list.

NOA 200302 (6-18 h)							WIA 200302 (6-18 h)						
obs→ ↓for	O1	O2	O3	O4	O5	sum	obs→ ↓for	O1	O2	O3	O4	O5	sum
F1	**922**	31	4	0	**1**	958	F1	**950**	26	3	0	**1**	980
F2	406	**48**	8	1	0	463	F2	379	**55**	12	1	0	447
F3	22	48	**42**	10	1	123	F3	20	46	**38**	8	1	113
F4	0	2	7	**1**	1	11	F4	1	2	8	**3**	1	15
F5	0	0	0	0	**0**	0	F5	0	0	0	0	**0**	0
sum	1350	129	61	12	3	1555	sum	1350	129	61	12	3	1555
%FO	68	37	69	8	0	65	%FO	70	43	62	25	0	67

NOA 200302 (18-30 h)							WIA 200302 (18-30 h)						
obs→ ↓for	O1	O2	O3	O4	O5	sum	obs→ ↓for	O1	O2	O3	O4	O5	sum
F1	**747**	18	3	0	**1**	769	F1	**728**	26	4	0	**1**	759
F2	565	**41**	10	2	0	618	F2	592	**54**	11	1	0	658
F3	37	67	**44**	9	2	159	F3	30	47	**41**	10	2	130
F4	1	3	4	**1**	0	9	F4	0	2	5	**1**	0	8
F5	0	0	0	0	**0**	0	F5	0	0	0	0	**0**	0
sum	1350	129	61	12	3	1555	sum	1350	129	61	12	3	1555
%FO	55	32	72	8	0	54	%FO	54	42	67	8	0	53

$1.0 \leq P3 < 5$, $5 \leq P4 < 10$ and $P5 \geq 10$. P is either F (forecast) or O (observation) in the tables. The "sum" row and column are the sum of numbers in the given observation class or forecast class, respectively. These tables show that precipitation forecasts are not improved in these two months since WIA is better with respect to some numbers and vice versa. Contingency tables for a Danish station list (when available: 06030, 06041, 06052, 06058, 06060, 06065, 06070, 06072 06074, 06079, 06080, 06081, 06102, 06104, 06108, 06110 06116, 06119, 06120, 06126, 06135, 06141, 06156, 06160 06170, 06180, 06190, 06193, 06197) are given in Tables 4 and 5. Here WIA is generally better than NOA. However, it should be noted that January and February were dry and accordingly only little statistics are available for larger precipitation amounts (the O4 and O5 classes) compared to the statistics for the EWGLAM station list.

4.2. Field verification

Figures 16 and 17 show differences in standard deviation fields of mslp and 850 hPa temperature for January and February 2003, respectively. These figures show that – in particular for mslp – larger areas with smaller standard deviation scores for WIA than for NOA. Over Europe this tendency is even more pronounced.

5. Conclusion

The results from January and February show a clear positive impact from using AMSU-A data from NOAA16 and NOAA17 compared to not using any AMSU-A data.

The example from November 2002 shows that the first guess check is important in the very rare occasions for which bad data are generated.

The new service by EUMETSAT (European Organisation for the Exploitation of Meteorological Satellites), EARS (EUMETSAT's ATOVS Retransmission Service), will provide additional ATOVS data besides the locally received data already in use. In particular, extra data in the southwestern part of the Atlantic will be available which could be important in some weather situations.

References

Amstrup, Bjarne. 2001. *Impact of ATOVS AMSU-A radiance data in the DMI-HIRLAM 3D-Var analysis and forecasting system.* DMI Scientific Report 01-06. Danish Meteorological Institute.

Amstrup, Bjarne, Mogensen, Kristian Sten, Nielsen, Niels Woetmann, Huess, Vibeke and Nielsen, Jacob Woge. 2003. *Results from DMI-HIRLAM pre-operational tests prior to the upgrade in December 2002.* DMI Technical Report 03-20. Danish Meteorological Institute.

Bouttier, F. and Kelly, G. 2001. Observing-system experiments in the ECMWF 4D-Var data assimilation system. *Quart. J. Roy. Meteorol. Soc.*, **127**, 1469–1488.

Gustafsson, N. and Svensson, J. 1988. A data assimilation experiment with high resolution TOVS data. *HIRLAM Technical Report*, **3**.

Gustafsson, N., Berre, L., Hörnquist, S., Huang, X.-Y., Lindskog, M., Navascués, B., Mogensen, K. S. and Thorsteinsson, S. 2001. Three-dimensional variational data assimilation for a limited area model. Part I: General formulation and the background error constraint. *Tellus*, **53A**, 425–446.

Lindskog, M., Gustafsson, N., Navascués, B., Mogensen, K. S., Huang, X.-Y., Yang, X., Andræ, U., Berre, L., Thorsteinsson, S. and Rantakokko, J. 2001. Three-dimensional variational data assimilation for a limited area model. Part II: Observation handling and assimilation experiments. *Tellus*, **53A**, 447–468.

Sass, Bent Hansen, Nielsen, Niels Woetmann, Jørgensen, Jess U., Amstrup, Bjarne, Kmit, Maryanne and Mogensen, Kristian S. 2002. *The Operational DMI-HIRLAM System - 2002 version*. DMI Technical Report 02-5. Danish Meteorological Institute.

Saunders, R., Matricardi, M. and Brunel, P. 1999. An improved fast radiative transfer model for assimilation of satellite radiance observations. *Quart. J. Roy. Meteorol. Soc.*, **125**, 1407–1425.

Schyberg, Harald, Landelius, Tomas, Thorsteinsson, Sigurdur, Tveter, Frank Thomas, Vignes, Ole, Amstrup, Bjarne, Gustafsson, Nils, Järvinen, Heikki and Lindskog, Magnus. 2003. Assimilation of ATOVS data in the HIRLAM 3D-VAR System. *HIRLAM Technical Report*, **60**.

WMO. 1995. *Manual on codes, Volume I, International codes, Part B - Binary codes*. No 306, fm-94-ix, ext. bufr edn.
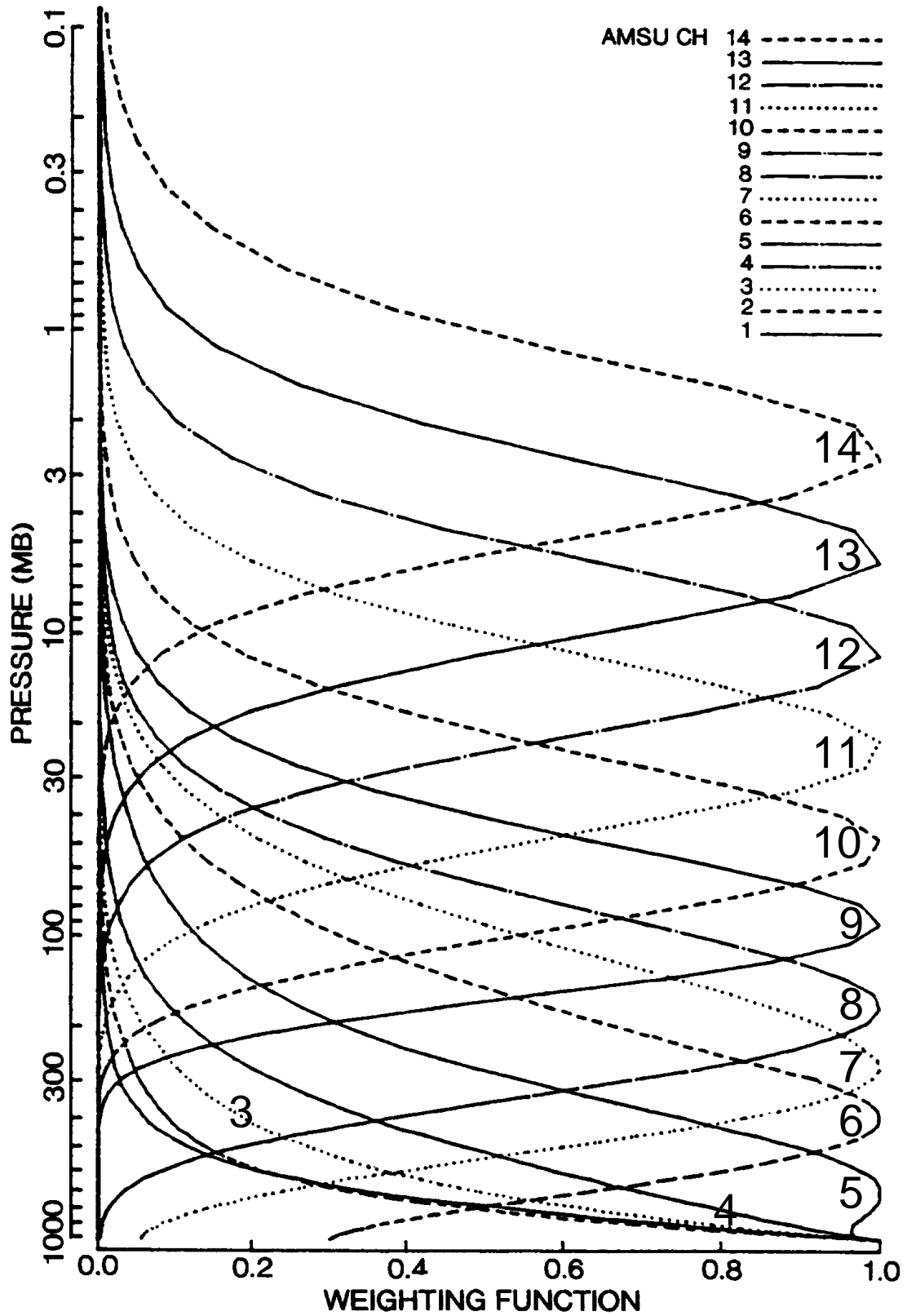
Figure 2: Normalized response/weighting functions for AMSU-A data. Each point corresponds to a data point. Figure taken from ECMWF notes for data assimilation course. (the notes are available under on `http://www.ecmwf.int/newsevents/training/` `rcourse_notes/`).
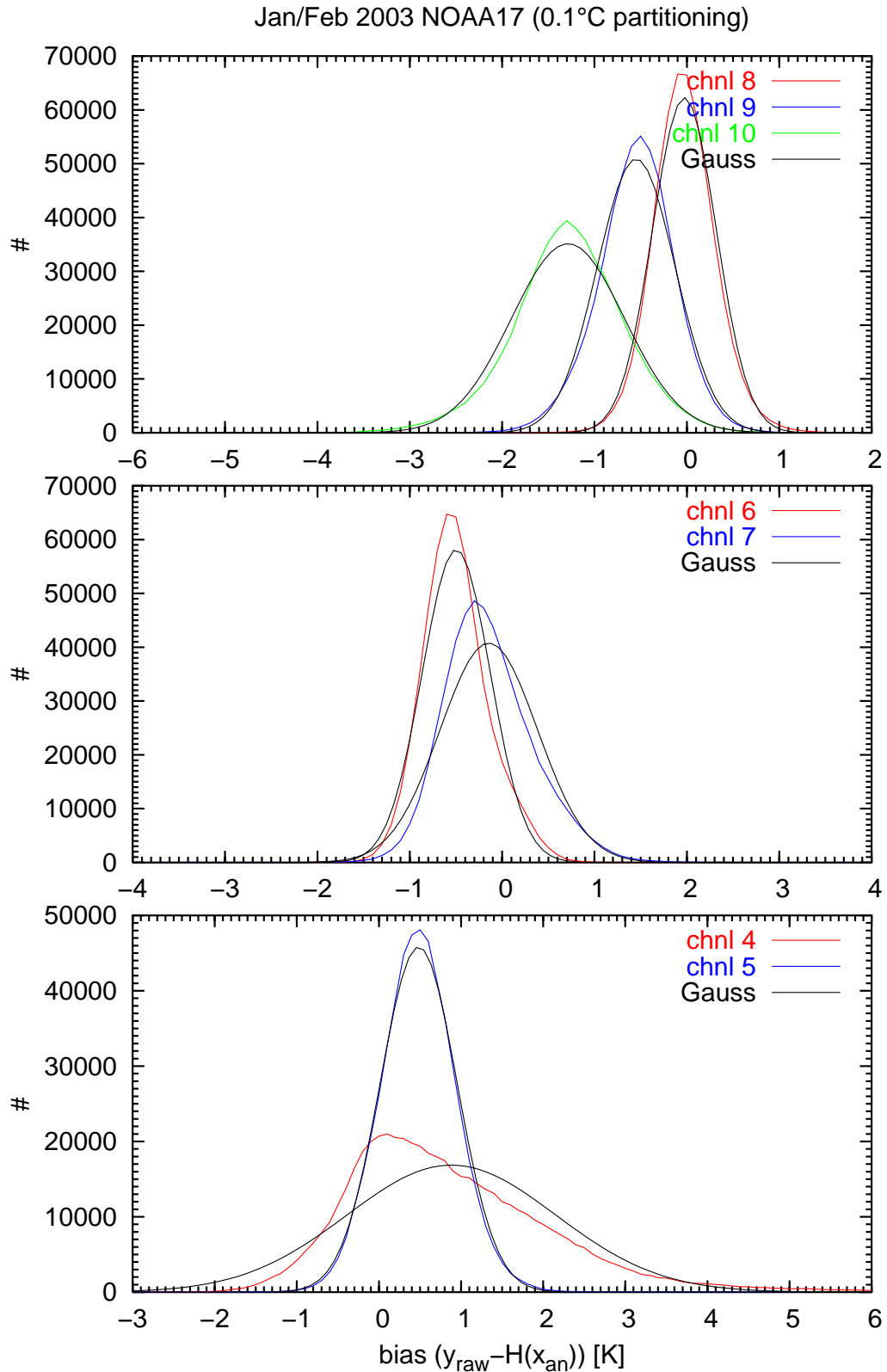
Figure 3: Partitioning of NOAA17 data from January/February 2003 according to the number of data with given differences (innovations) between observed brightness temperature (y_{raw}) and the modeled one ($H(\mathbf{x}_{\mathrm{an}})$). Overlayed is the "best fit" Gaussian distribution.
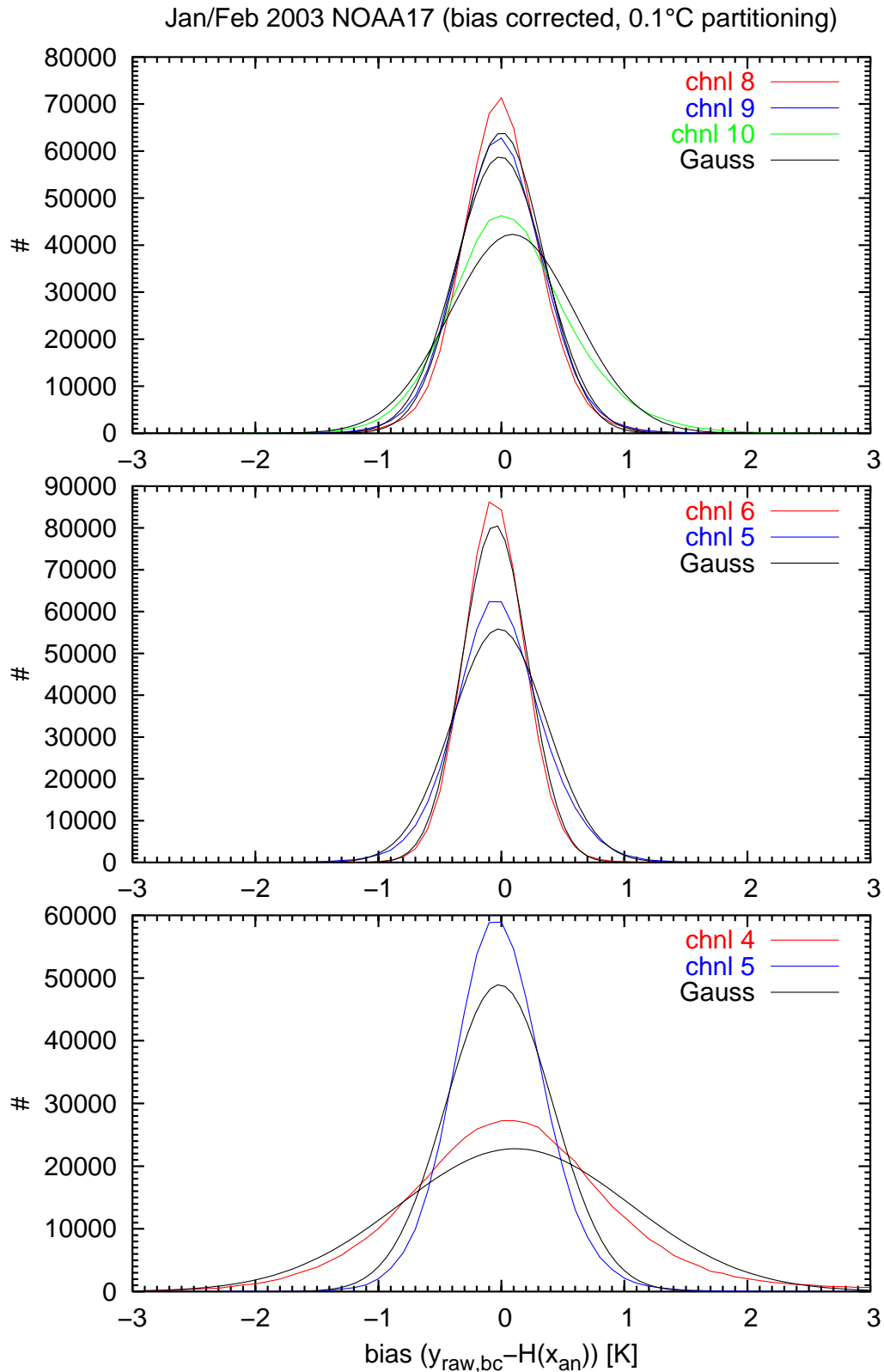
Figure 4: Partitioning of NOAA17 data from January/February 2003 according to the number of data with given differences (innovations) between bias corrected observed brightness temperature ($y_{\mathrm{raw,bc}}$) and the modeled one ($H(\mathbf{x}_{\mathrm{an}})$). Overlayed is the "best fit" Gaussian distribution.
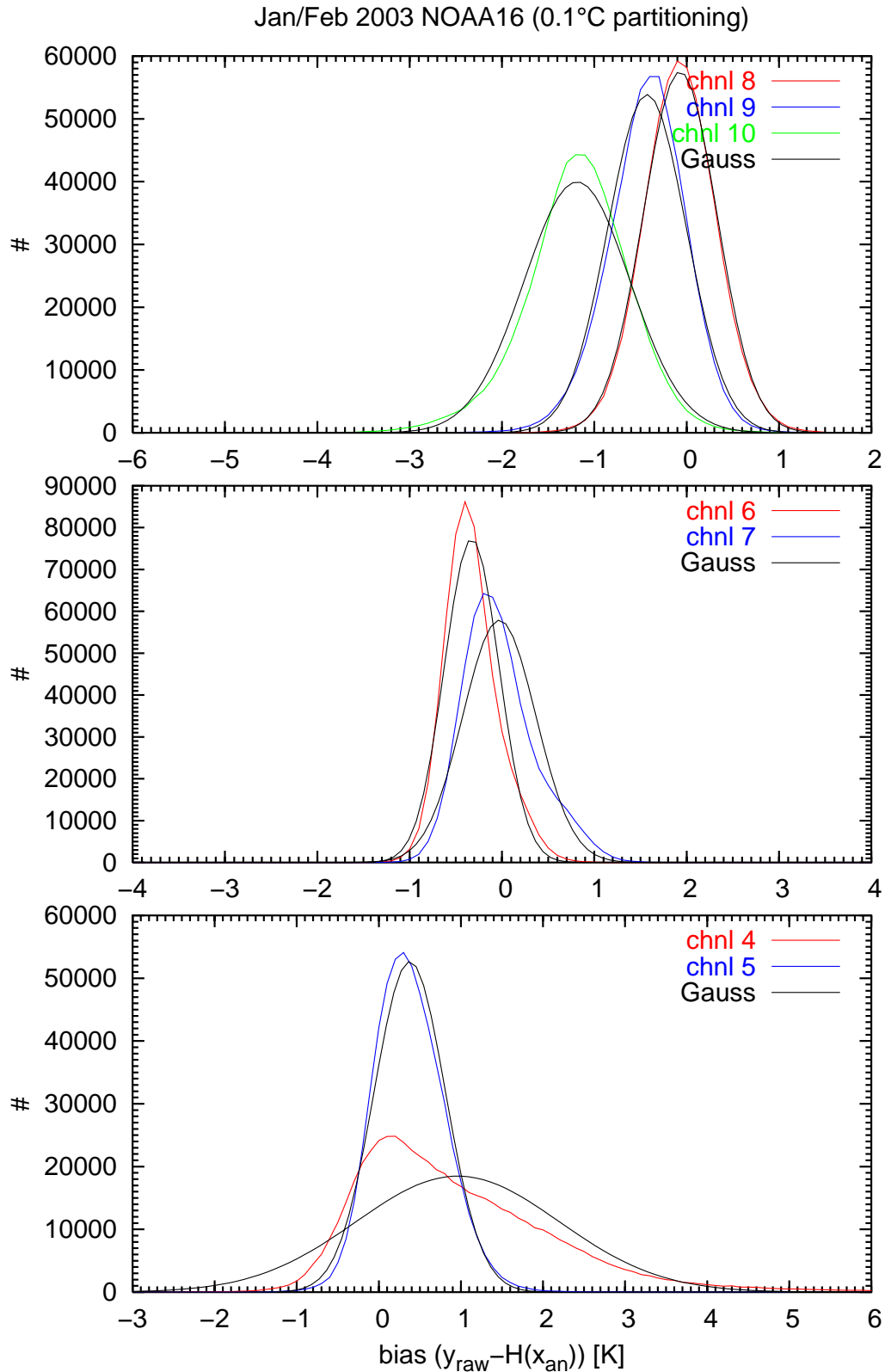
Figure 5: Partitioning of NOAA16 data from January/February 2003 according to the number of data with given differences (innovations) between observed brightness temperature (y_{raw}) and the modeled one ($H(\mathbf{x}_{\mathrm{an}})$). Overlayed is the "best fit" Gaussian distribution.
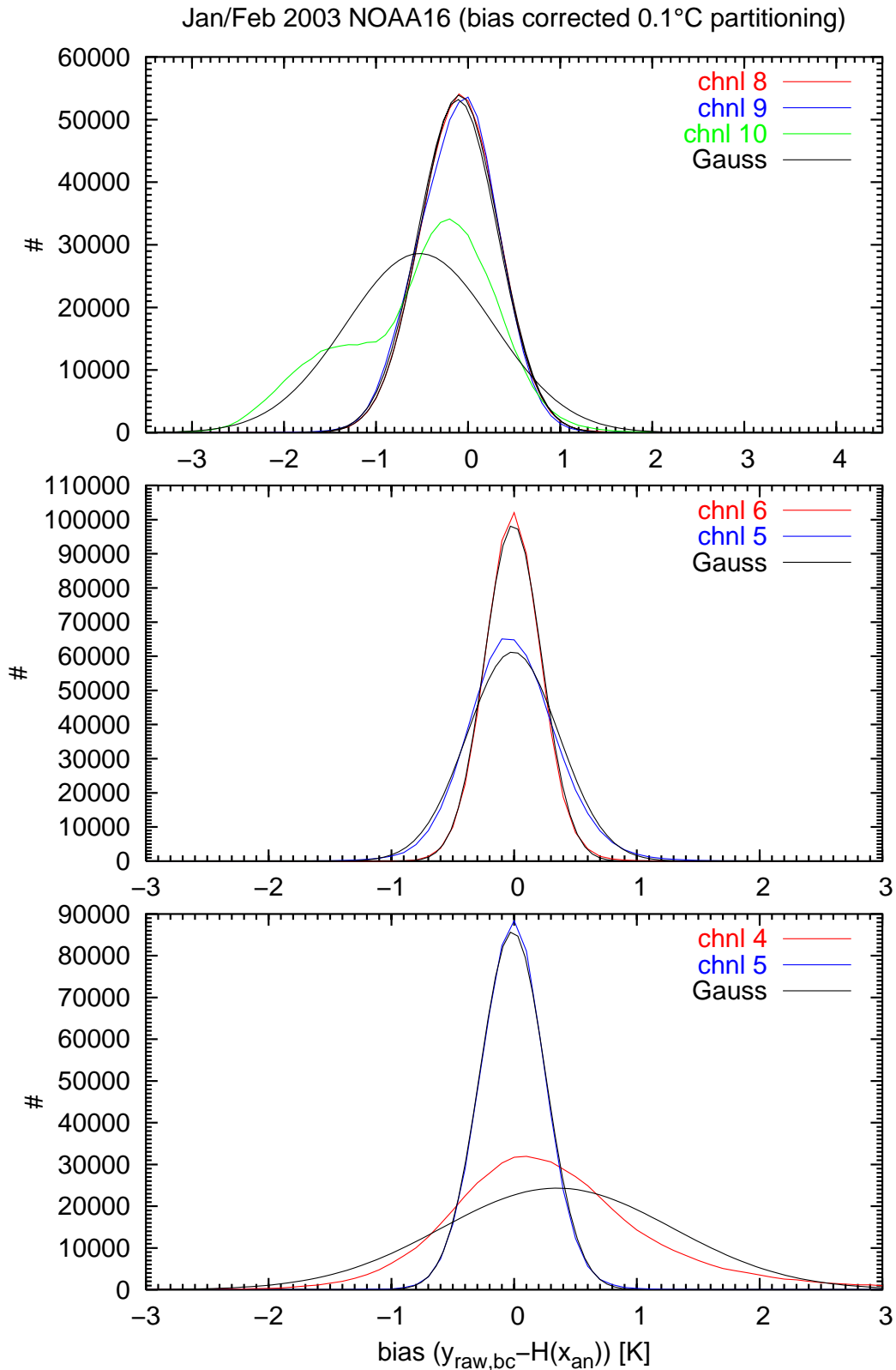
Figure 6: Partitioning of NOAA16 data from January/February 2003 according to the number of data with given differences (innovations) between bias corrected observed brightness temperature ($y_{\mathrm{raw,bc}}$) and the modeled one ($H(\mathbf{x}_{\mathrm{an}})$). Overlayed is the "best fit" Gaussian distribution.
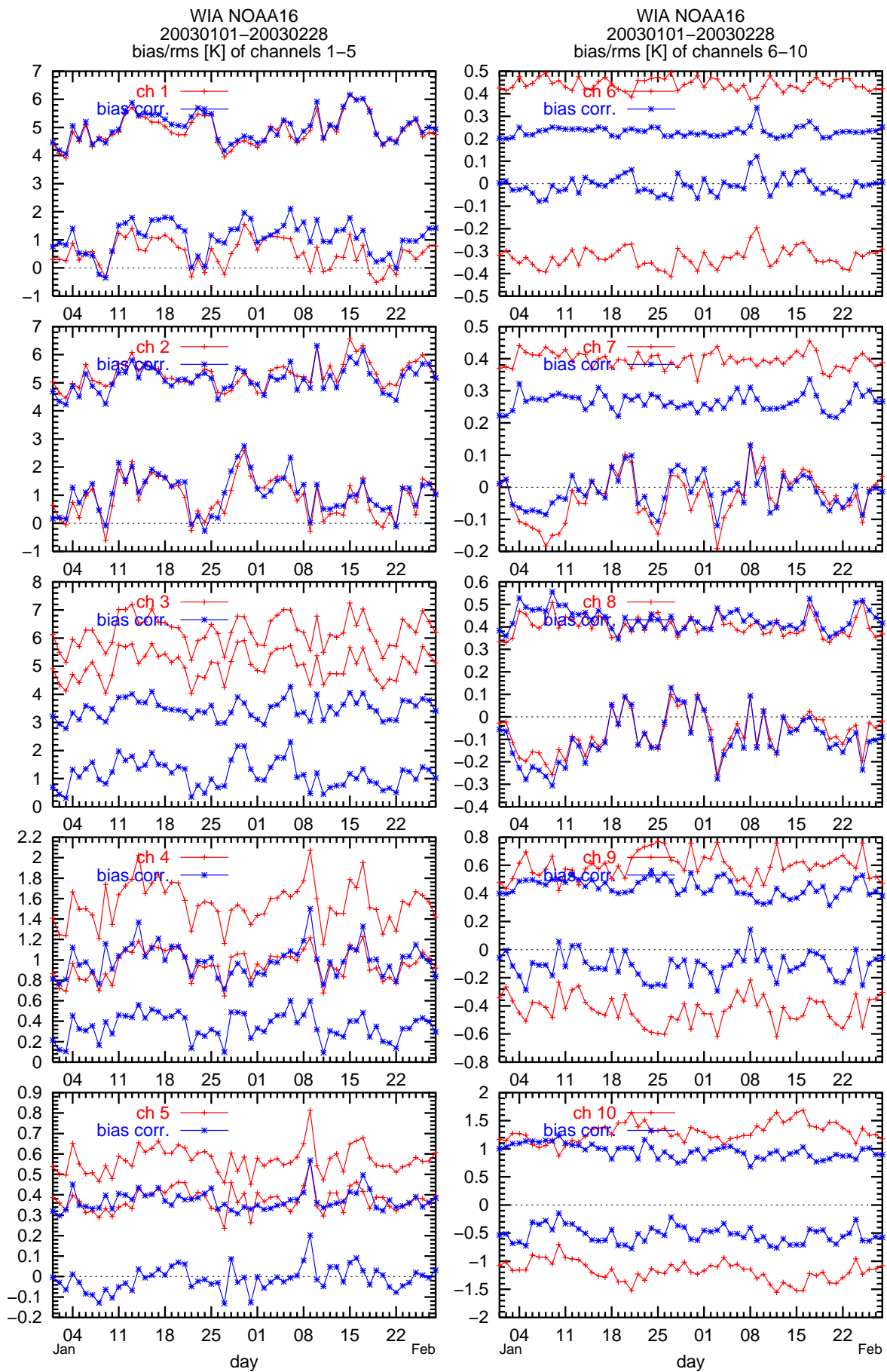
Figure 7: Daily bias- and rms-values (level 1c (OBS − AN) brightness temperature departure (in K)) for NOAA16 AMSU-A channels 1-10 in January and February 2003. In average 9733 values are included in the statistics per day for channels 4 to 10. Red values for uncorrected and blue for bias corrected values.

17
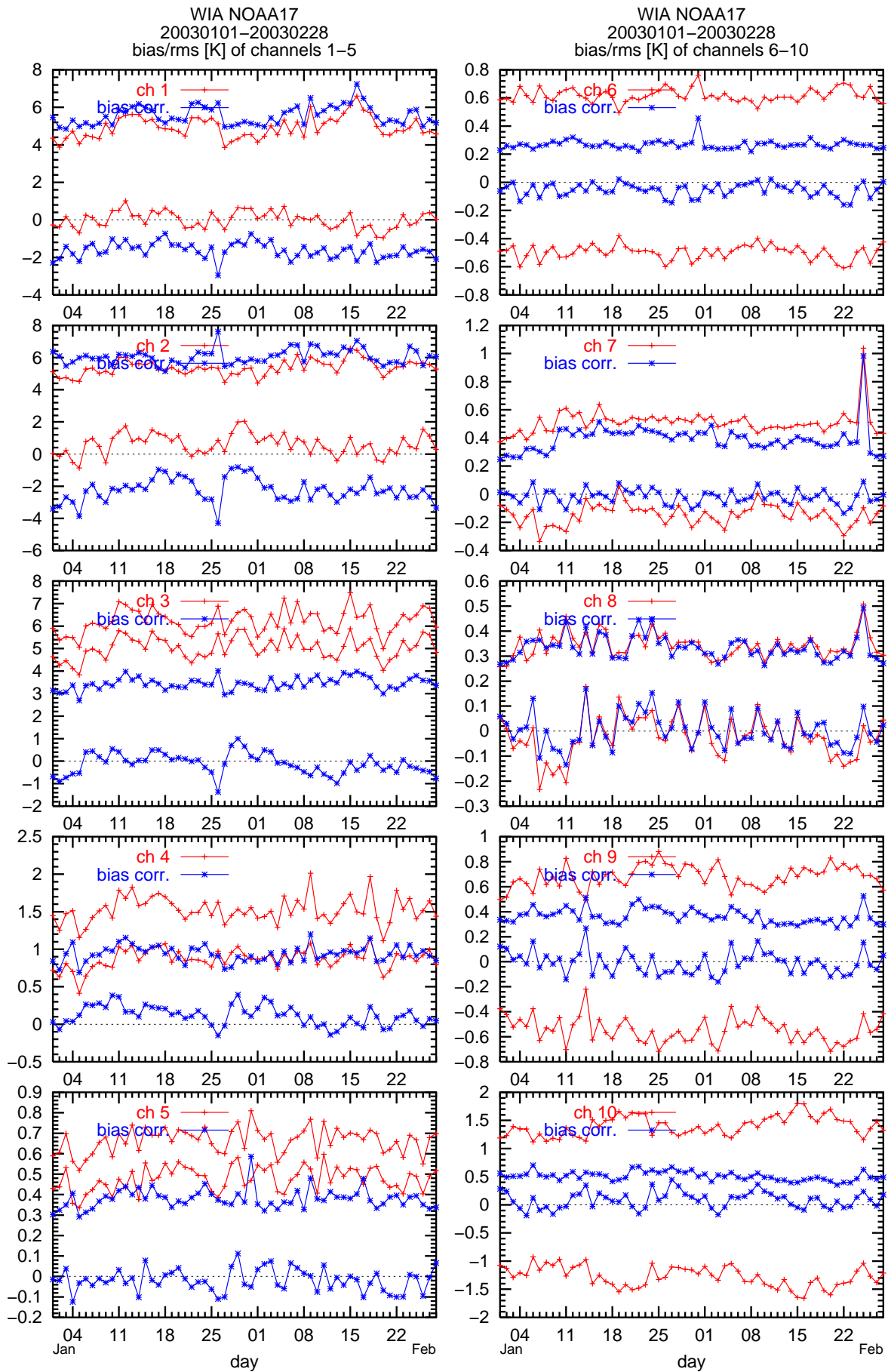
Figure 8: Daily bias- and rms-values (level 1c (OBS − AN) brightness temperature departure (in K)) for NOAA17 AMSU-A channels 1-10 in January and February 2003. In average 9122 values are included in the statistics per day for channels 4 to 10. Red values for uncorrected and blue for bias corrected values.

18
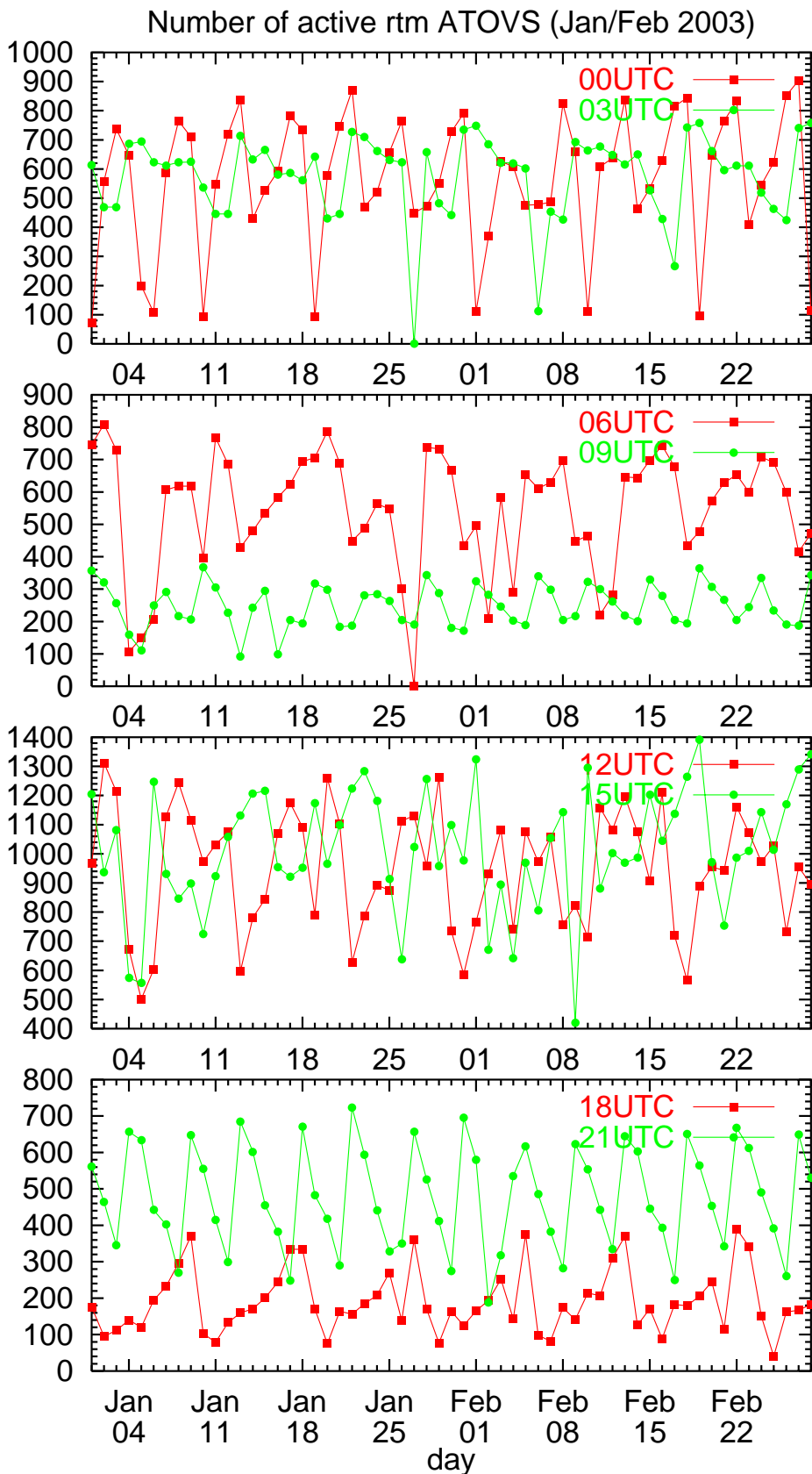
Figure 9: Number of active rtm ATOVS during January and February 2003 for the given analysis cycles (00 UTC and 03 UTC upper, 06 UTC and 09 UTC upper middle, 12 UTC and 15 UTC lower middle, and 18 UTC and 21 UTC bottom).

19
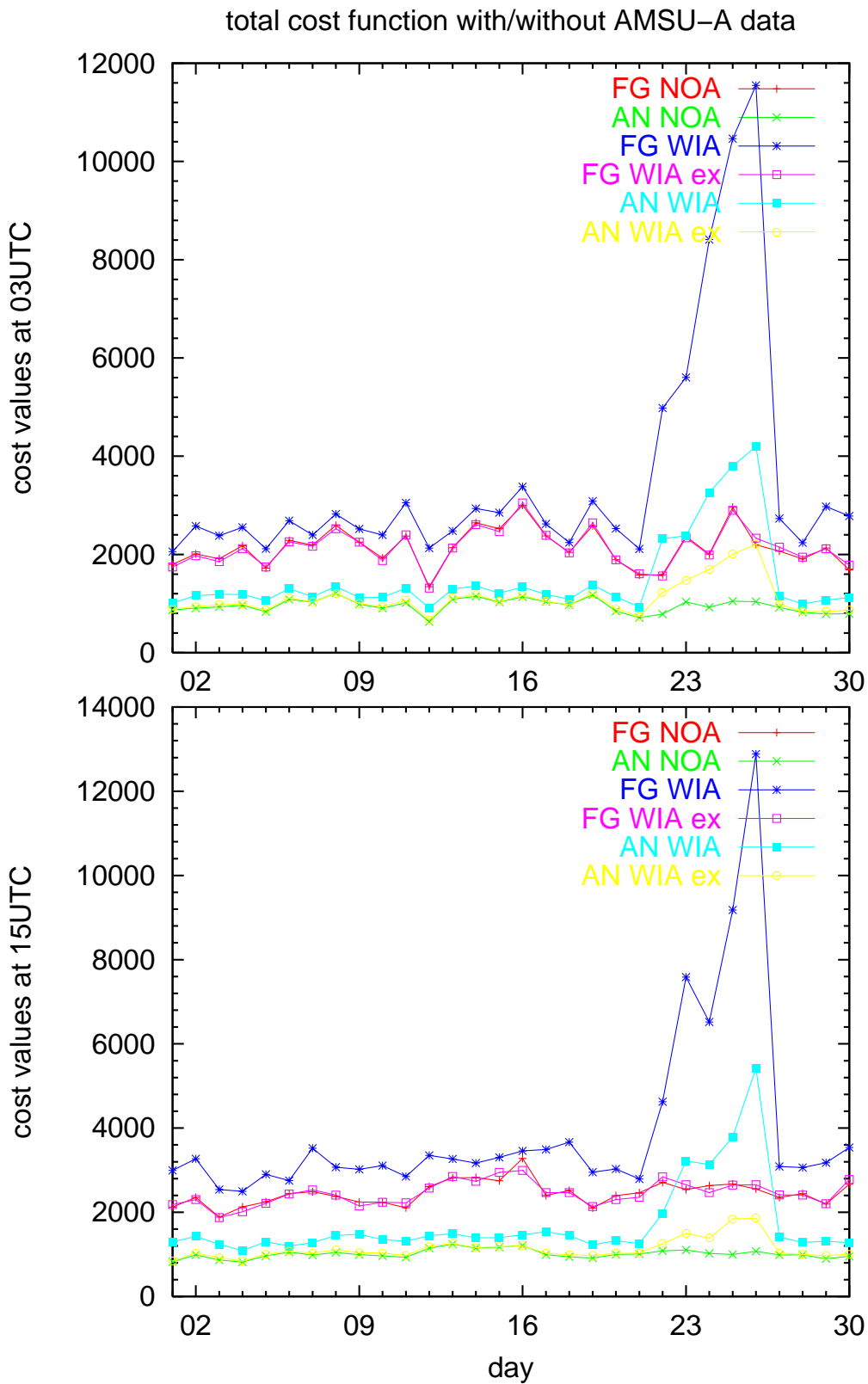
Figure 10: Cost function values for 03 UTC analyses and 15 UTC analyses in November 2002. "FG NOA" stands for first guess values for the model run without inclusion of AMSU-A data and "AN NOA" is the same except for being the analysis value. Similarly "FG WIA" and "AN WIA" are for the run with inclusion of AMSU-A data. "FG WIA ex" and "AN WIA ex" are the total cost function for the model run with inclusion of AMSU-A data minus the AMSU-A part of cost function value. Note that "FG NOA" and "FG WIA ex" are very close in the plots except from the 21st to 26th.

20
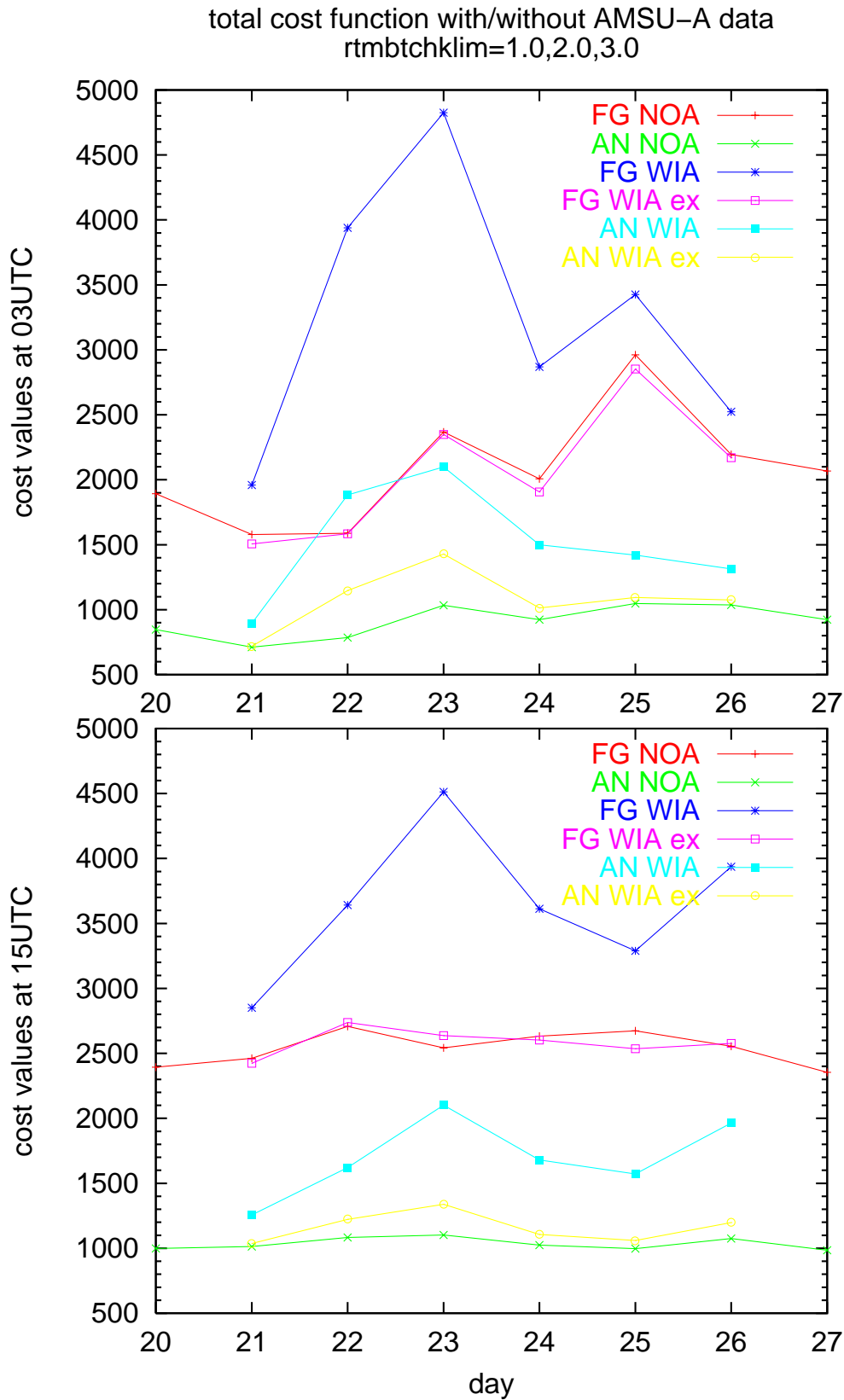
Figure 11: Cost function values for 03 UTC analyses and 15 UTC analyses in the period in November 2002 for the rerun with reduced rtmbtchklim values. "FG NOA" stands for first guess values for the model run without inclusion of AMSU-A data and "AN NOA" is the same except for being the analysis value. Similarly "FG WIA" and "AN WIA" are for the run with inclusion of AMSU-A data. "FG WIA ex" and "AN WIA ex" are the total cost function for the model run with inclusion of AMSU-A data minus the AMSU-A part of cost function value.
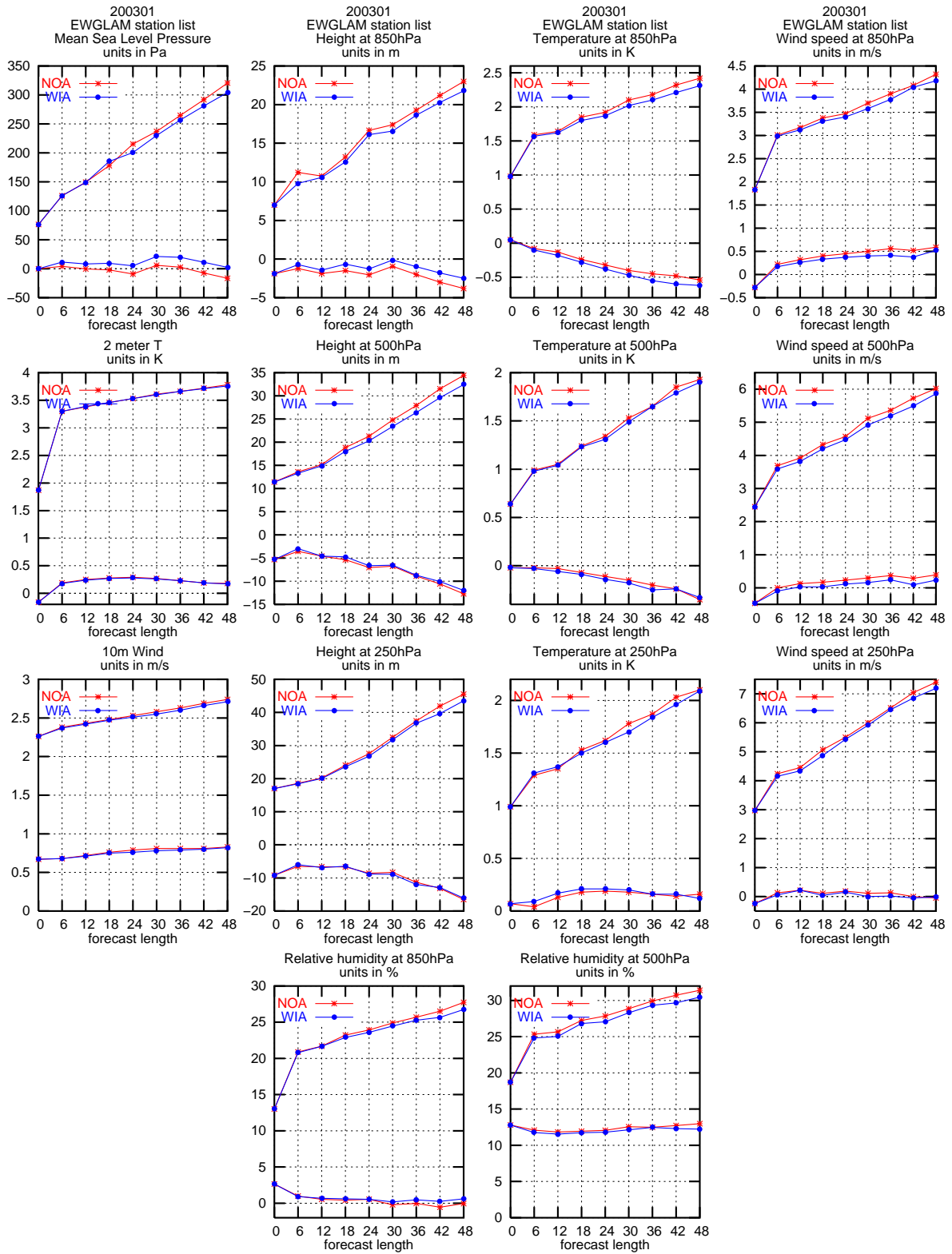
Figure 12: Obs-verification (bias and rms, EWGLAM station list) results for January 2003 of surface parameters and geopotential height, temperature, humidity and wind for pressure levels specified in the plot. ECMWF analyses have been used to reject observations and the analysis verification scores are for ECMWF.
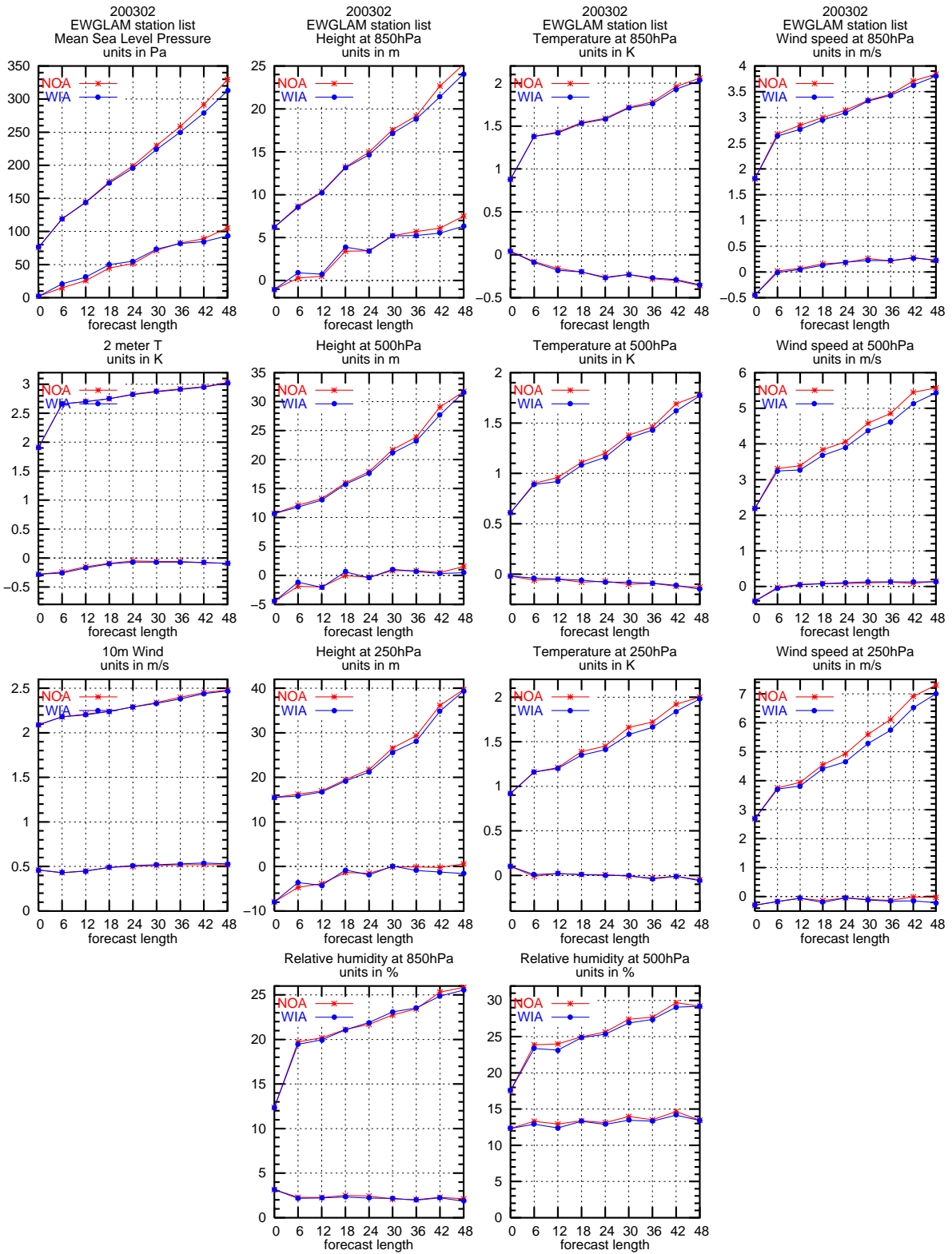
Figure 13: Obs-verification (bias and rms, EWGLAM station list) results for February 2003 of surface parameters and geopotential height, temperature, humidity and wind for pressure levels specified in the plot. ECMWF analyses have been used to reject observations and the analysis verification scores are for ECMWF.
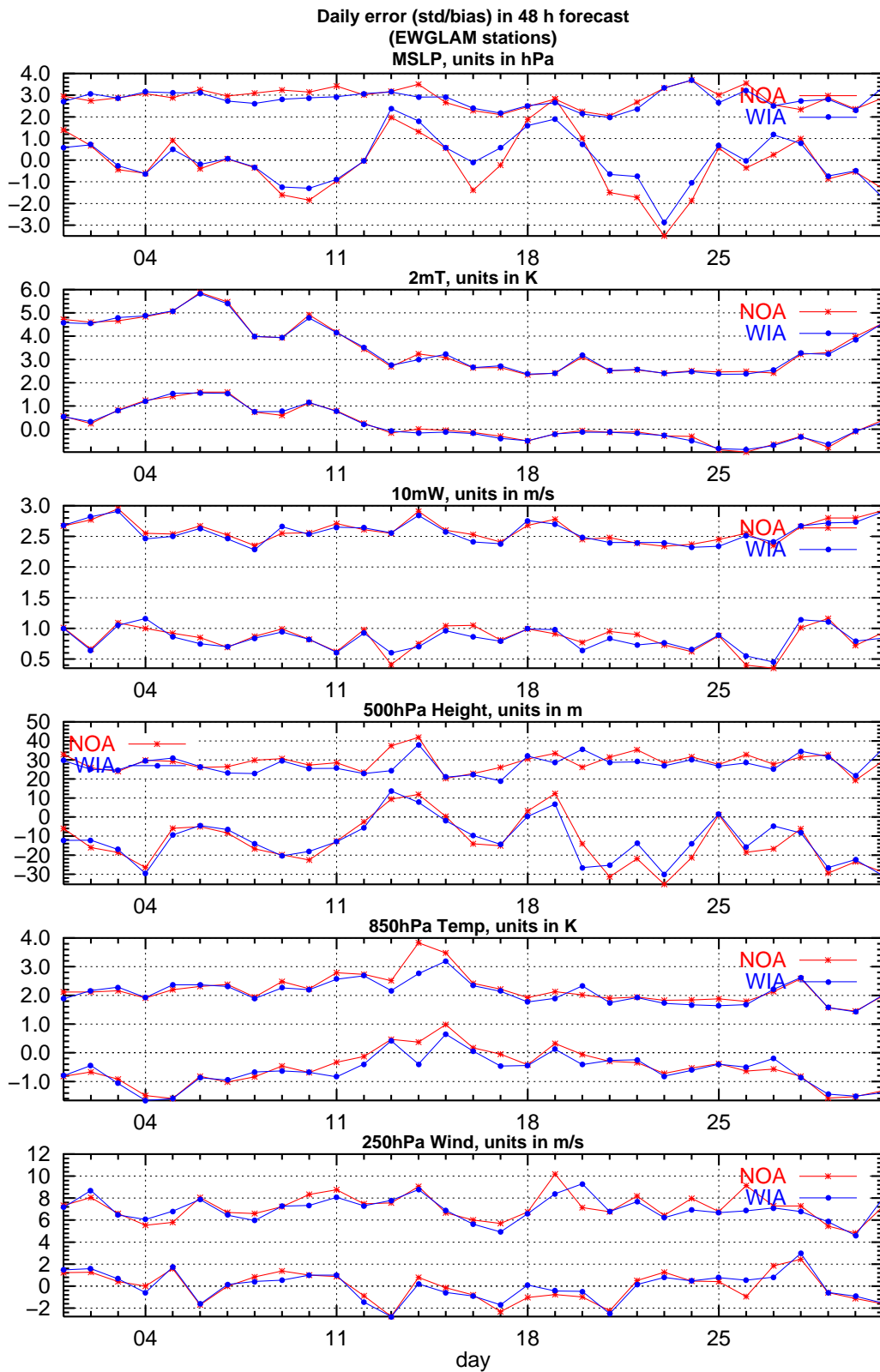
Figure 14: Daily obs-verification (bias and standard deviation, EWGLAM station list) results of 48 h forecasts for January 2002 of surface and upper level parameters specified in the plot.
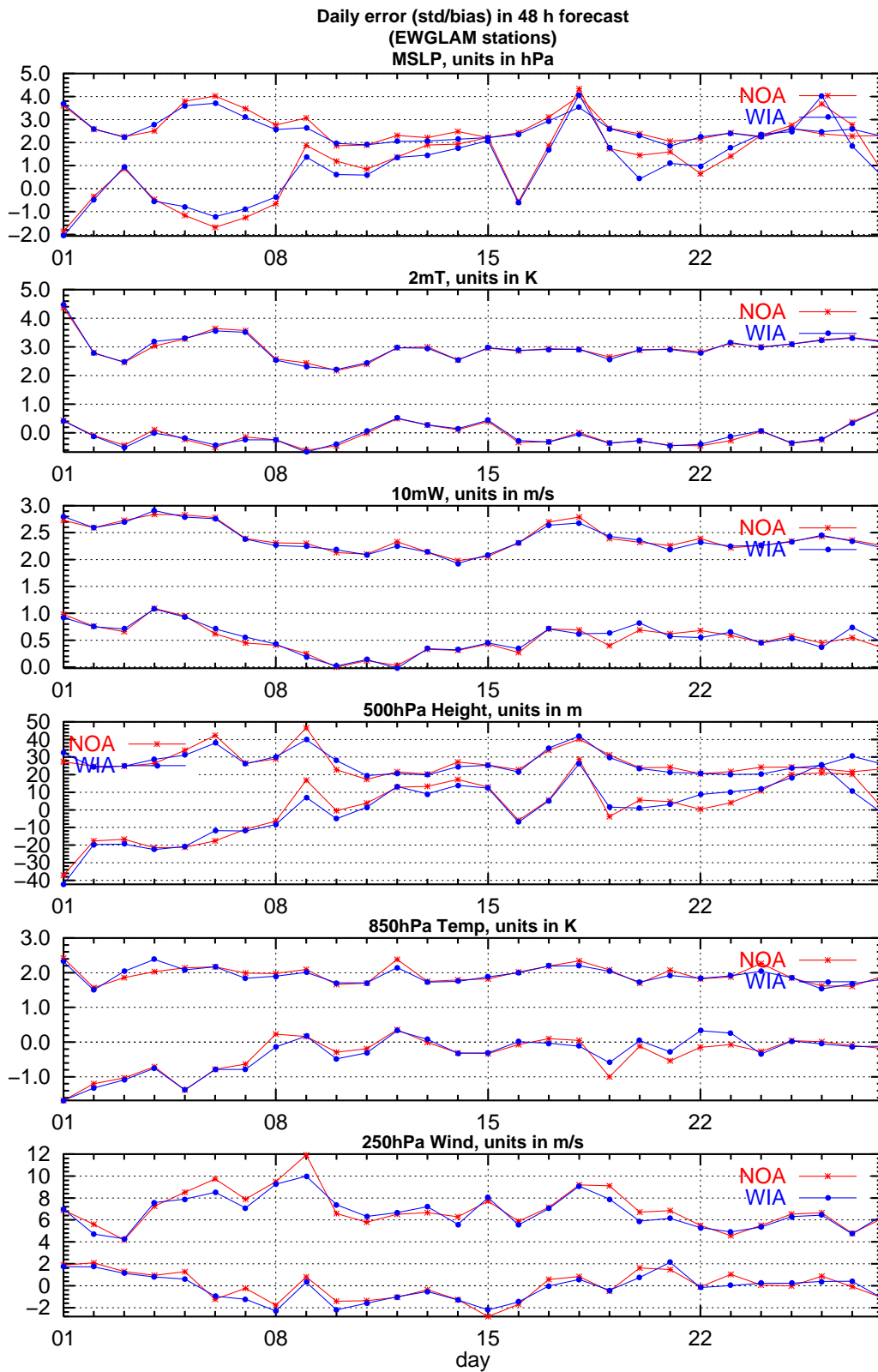
Figure 15: Daily obs-verification (bias and standard deviation, EWGLAM station list) results of 48 h forecasts for February 2002 of surface and upper level parameters specified in the plot.
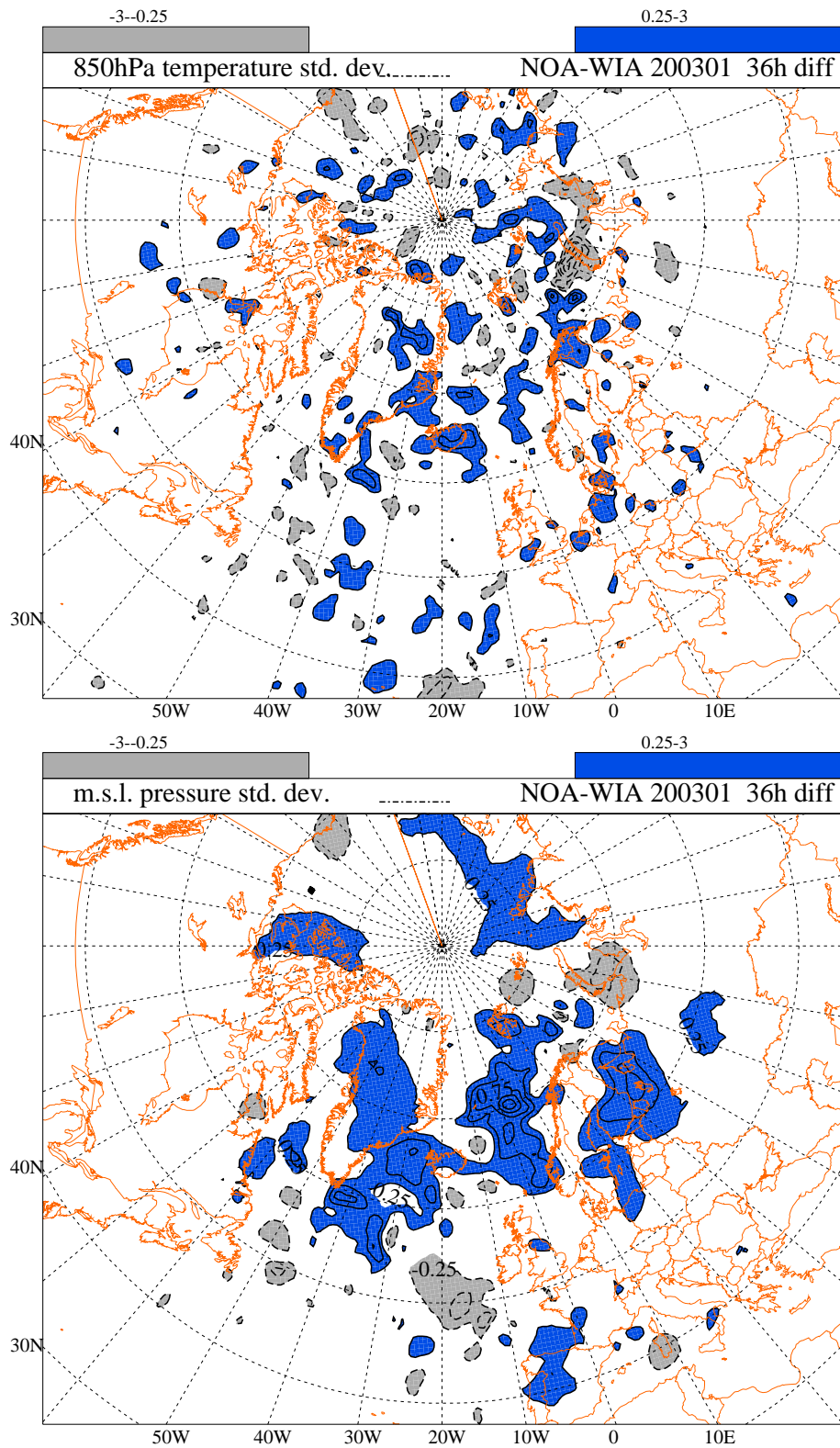
Figure 16: Difference of standard deviation between the NOA (analyses not including AMSU-A brightness temperatures) and the WIA (analyses including AMSU-A brightness temperatures) for 36 h forecasts of 850 hPa temperature (upper) and mslp (lower) for January 2003. Full lines/blue shaded for areas where WIA is better and dashed lines/grey shaded for areas where NOA has better standard deviation scores. Contour lines are for every 0.25 K and 0.25 hPa, respectively.

26
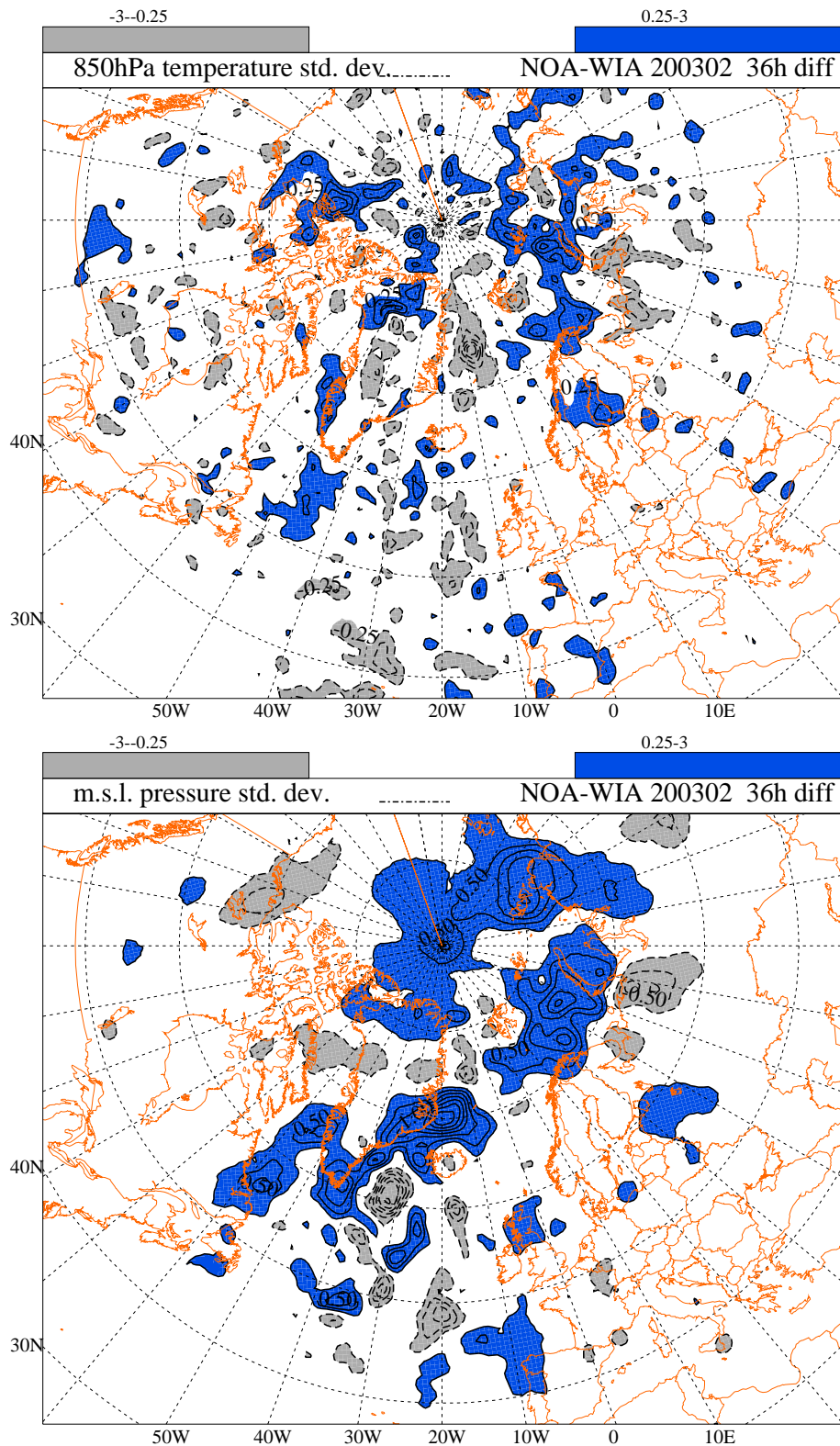
Figure 17: Difference of standard deviation between the NOA (analyses not including AMSU-A brightness temperatures) and the WIA (analyses including AMSU-A brightness temperatures) for 36 h forecasts of 850 hPa temperature (upper) and mslp (lower) for February 2003. Full lines/blue shaded for areas where WIA is better and dashed lines/grey shaded for areas where NOA has better standard deviation scores. Contour lines are for every 0.25 K and 0.25 hPa, respectively.

DANISH METEOROLOGICAL INSTITUTE

Scientific Reports

Scientific reports from the Danish Meteorological Institute cover a variety of geophysical fields, i.e. meteorology (including climatology), oceanography, subjects on air and sea pollution, geomagnetism, solar-terrestrial physics, and physics of the middle and upper atmosphere.

Reports in the series within the last five years:

No. 97-1
E. Friis Christensen og C. Skøtt: Contributions from the International Science Team. The Ørsted Mission - a pre-launch compendium

No. 97-2
Alix Rasmussen, Sissi Kiilsholm, Jens Havskov Sørensen, Ib Steen Mikkelsen: Analysis of tropospheric ozone measurements in Greenland: Contract No. EV5V-CT93-0318 (DG 12 DTEE):
DMI's contribution to CEC Final Report Arctic Trophospheric Ozone Chemistry ARCTOC

No. 97-3
Peter Thejll: A search for effects of external events on terrestrial atmospheric pressure: cosmic rays

No. 97-4
Peter Thejll: A search for effects of external events on terrestrial atmospheric pressure: sector boundary crossings

No. 97-5
Knud Lassen: Twentieth century retreat of sea-ice in the Greenland Sea

No. 98-1
Niels Woetman Nielsen, Bjarne Amstrup, Jess U. Jørgensen: HIRLAM 2.5 parallel tests at DMI: sensitivity to type of schemes for turbulence, moist processes and advection

No. 98-2
Per Høeg, Georg Bergeton Larsen, Hans-Henrik Benzon, Stig Syndergaard, Mette Dahl Mortensen: The GPSOS project
Algorithm functional design and analysis of ionosphere, stratosphere and troposphere observations

No. 98-3
Mette Dahl Mortensen, Per Høeg: Satellite atmosphere profiling retrieval in a nonlinear troposphere
Previously entitled: Limitations induced by Multipath

No. 98-4
Mette Dahl Mortensen, Per Høeg: Resolution properties in atmospheric profiling with GPS

No. 98-5
R.S. Gill and M. K. Rosengren: Evaluation of the Radarsat imagery for the operational mapping of sea ice around Greenland in 1997

No. 98-6
R.S. Gill, H.H. Valeur, P. Nielsen and K.Q. Hansen: Using ERS SAR images in the operational mapping of sea ice in the Greenland waters: final report for ESA-ESRIN's: pilot projekt no. PP2.PP2.DK2 and 2nd announcement of opportunity for the exploitation of ERS data projekt No. AO2..DK 102

No. 98-7
Per Høeg et al.: GPS Atmosphere profiling methods and error assessments

No. 98-8
H. Svensmark, N. Woetmann Nielsen and A.M. Sempreviva: Large scale soft and hard turbulent states of the atmosphere

No. 98-9
Philippe Lopez, Eigil Kaas and Annette Guldberg: The full particle-in-cell advection scheme in spherical geometry

No. 98-10
H. Svensmark: Influence of cosmic rays on earth's climate

No. 98-11
Peter Thejll and Henrik Svensmark: Notes on the method of normalized multivariate regression

No. 98-12
K. Lassen: Extent of sea ice in the Greenland Sea 1877-1997: an extension of DMI Scientific Report 97-5

No. 98-13
Niels Larsen, Alberto Adriani and Guido DiDonfrancesco: Microphysical analysis of polar stratospheric clouds observed by lidar at McMurdo, Antarctica

No.98-14
Mette Dahl Mortensen: The back-propagation method for inversion of radio occultation data